Structural Organization and Transport Properties of iPP/LLDPE Blends Solidified at Controlled Cooling Rates

IVANO COCCORULLO, GIULIANA GORRASI, ROBERTO PANTANI

Dipartimento di Ingegneria Chimica e Alimentare, Università di Salerno, Via Ponte don Melillo, 84084 Fisciano, Salerno, Italy

ABSTRACT: The structural organization of blends of isotactic polypropylene (iPP) and linear low-density polyethylene (LLDPE), with different compositions, was studied and correlated with the thermal history followed by the samples during solidification from the molten state. The materials were cooled at two extreme controlled rates: 0.1 and 500°C/s. The resulting structure was investigated both in the crystalline and the amorphous phases. In particular, attention was focused toward the analysis of the diffusion parameters of dichloromethane vapors, and the morphological organization of the amorphous phases was interpreted using models that consider them (in terms of resistance to diffusion) combined in series and in parallel. © 2001 John Wiley & Sons, Inc. J Appl Polym Sci 82: 2237–2244, 2001

Key words: blends; polyethylene; poly(propylene); diffusion

INTRODUCTION

Polymeric materials are often quite complex as they include several phases, each of them being optimized to improve either processing performance or final product properties. The study of the solidification of polymers in processing conditions is limited by the fact that standard tests to describe the polymer volume during cooling are confined to unreasonably low cooling rates and/or pressure, if compared with those experienced by the material during processing. Indeed, conventional experimental techniques used to follow the solidification from the melt (as, for instance, differential scanning calorimetry) are able to cover satisfactorily a small range of rate of cooling, generally not higher than 100°C/min. In most cases, the industrial processes need much higher cooling rates. In some processes, such as injection mold-ing, during solidification, the material experiences cooling rates that range from hundreds of degrees per second (close to the mold wall) to a minimum at the sample center, which is usually about 10°C per second. This induces a severe change in the properties and morphology along with the product thickness.[1–2] The simulation of the processing conditions is one of the crucial steps for understanding the structural organization and morphology of homopolymers and blends. It has been demonstrated that the structure developing during the processing is responsible for the physical properties of the manufacture.[3–5] In recent years, great attention has been addressed to theoretical and practical aspects of polymer blends, in particular, to polyethylene (PE) and isotactic polypropylene (iPP), which are the thermoplastics of highest consumption, due to their special and varied physical and mechanical properties. Furthermore, polyolefin blends attract additional interest due to the possibility of recycling plastic wastes.

Several factors influence the structural organization of a blend: (1) the chemical nature of the component polymers; (2) their chemical and physical parameters, that is, the molecular weight and molecular weight distribution, viscosity, and degree of tacticity (if present); (3) the composition of the blend; and (4) processing parameters, mainly in terms of the thermal history which the material undergoes. In the case of crystallizable polymers, the last point is of fundamental importance in determining the final characteristics of the samples, that is, the morphology (distribution of crystalline and amorphous dominions) being strictly dependent on the cooling conditions. A number of fundamental studies have been reported regarding the mechanical properties and crystallization kinetics of PE–polypropylene (PP) blends. High-density PE, low-density PE, and iPP are described as immiscible and composed of segregated crystalline phases of both PE and PP.[6–13] However, it is not clear from any work in the literature what happens in the amorphous phases. On the other hand, the thermodynamic state and the morphology of the amorphous phase play a fundamental role in determining the physical properties exhibited by the materials. It is therefore important to achieve the best description of this phase in both the segregated dominions and in their boundaries. Transport properties of vapors in polymers are very sensitive to the thermodynamic state of the amorphous phase. They have often been used for studying the amorphous component in polymers, both oriented and after drawing, showing the big potentialities of this technique in evidencing even small differences in the amorphous phases.[14–17]

In this paper, we report results concerning the study of the structural and morphological organization of blends of iPP and linear low-density polyethylene (LLDPE), solidified under two extreme controlled cooling histories. Attention was focused toward the amorphous component through analysis of the diffusion parameters. A small interacting molecule such as dichloromethane, already used as a model molecule in many structural studies,[16,17] was utilized. Experimental data were compared with the two simple models obtained, considering the amorphous phases as resistances to diffusion combined either in series or in parallel, or, in a more complex way, consisting of a combination of the two.

EXPERIMENTAL

Materials

The materials used in the present work were an LLDPE of M_n 67,551 and M_w 335,185 produced by Montell (Ferrara, Italy) and an iPP of M_n 36,000 and M_w 268,000, supplied by Statoil (Statchele, Norway). Blends of LLDPE/iPP, with the composition 75/25, 50/50, and 25/75 w/w (%), were prepared in the molten state at a high temperature (200°C) using a Brabender CO DECODER blender, equipped with rotating blades.

Controlled Quenching of Thin Samples

Characterized solidification quenches of thin polymer films were performed using a recently developed technique.[18] Thermal histories experienced by the samples were measured during the quenching process using a thin thermocouple connected to a fast data-acquisition system. A scheme of the experimental apparatus adopted for the cooling procedure is depicted in Figure 1. It consists of a sample holder made by two thin copper slabs linked to a rod which can slide vertically, bringing the sample from an oven, in the upper part of the apparatus, to the lower part, where a cooling fluid is sprayed against the copper slabs. The two copper slabs were 0.5 mm thick and the thickness of the polymer sample located between them was always about 0.1 mm; contact between the copper walls and the polymer was ensured by using elastic pincers. Temperature evolution was monitored by a thin thermocouple located inside the copper holders close to the polymer sample. Values of the Biot number were estimated smaller than 0.1 (up to the highest cooling rate attained) with reference to both the polymer sample and the copper holder. These values of the Biot number suggest that internal resistance to heat transfer is negligible with respect to the external one, and, thus, thermocouple readings can be considered representative of a homogeneous temperature inside the polymer.

Samples were kept in the "oven" at 230°C for 30 min and then cooled in the "bath" to room temperature. Two different thermal histories were imposed on the samples with this procedure: one of them with cooling rates of about 0.1°C/s (in the temperature interval 70–100°C), which will be referred to as "slow" cooling in the following, and the other one reaching about 500°C/s (in the temperature interval 70–100°C), which will be
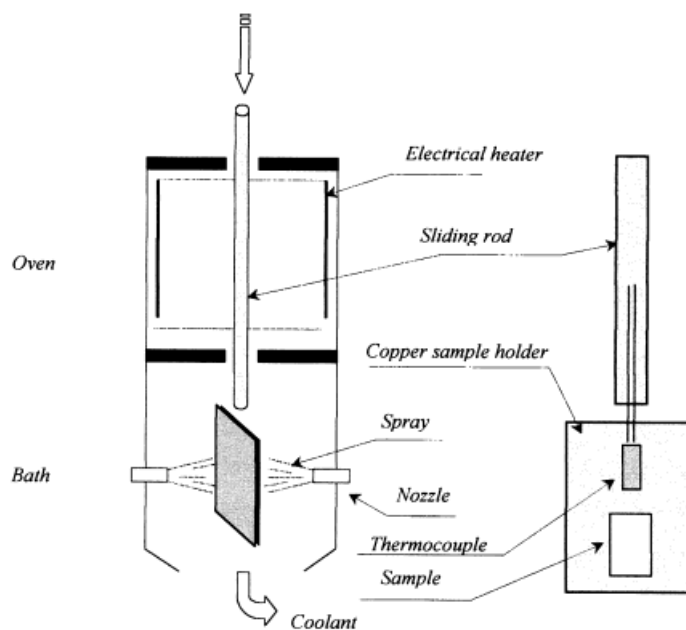
Figure 1 Experimental apparatus for controlled quenching of thin samples.

referred to as "fast" cooling in the following. Cooling rates monitored for pure polymers and their blends are reported in Figure 2 versus temperature. In the following, samples are coded by reporting the cooling rate ("*f*" for fast and "*s*" for slow) and the composition of the blend: For instance, a sample coded "fPE25-PP75" will refer to a sample solidified at 500°C/s whose weight composition is 25% of PE and 75% of iPP.

Methods of Investigation

Wide-angle X-ray diffractograms (WAXDs) were obtained using a PW 1050 Philips powder diffractometer (CuKα + Ni-filtered radiation). The scan rate was 2°θ/min.
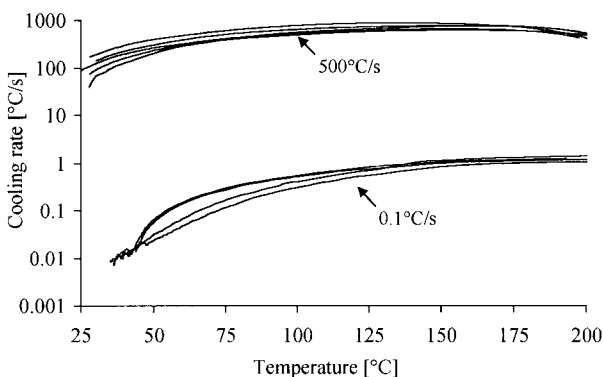

Figure 2 Cooling rates during sample solidification.

The density of all samples solidified was measured 1 h after solidification in density-gradient columns prepared with solutions of ethyl alcohol and water and conditioned at 25°C. Diffusion coefficients were evaluated, using the microgravimetric method.[16] The samples were put into a microgravimetric balance at different vapor activities of dichloromethane ($a = P/P_0$, where P is the actual pressure to which the sample was exposed, and P_0, the saturation pressure at the test temperature) at the temperature of 25°C. The gain in weight was followed as function of time up to the equilibrium.

RESULTS AND DISCUSSION

Structural Organization of the Blends

In Figure 3, WAXDs of samples submitted to slow cooling (0.1°C/s) are reported. The diffractogram of pure PE (sPE100-PP0) shows the main peaks at 21.4° and 23.8° of 2θ, characteristic of the orthorhombic structure. The diffractogram of pure iPP (sPE0-PP100) shows the main peaks at 14.1°, 16.8°, and 18.4° of 2θ, characteristic of the monoclinic α form. All these peaks are well identified also in the blends and their relative intensities are proportional to the amount of the two polymers present in the blend. This result can be taken as an evidence that, at slow cooling rates,
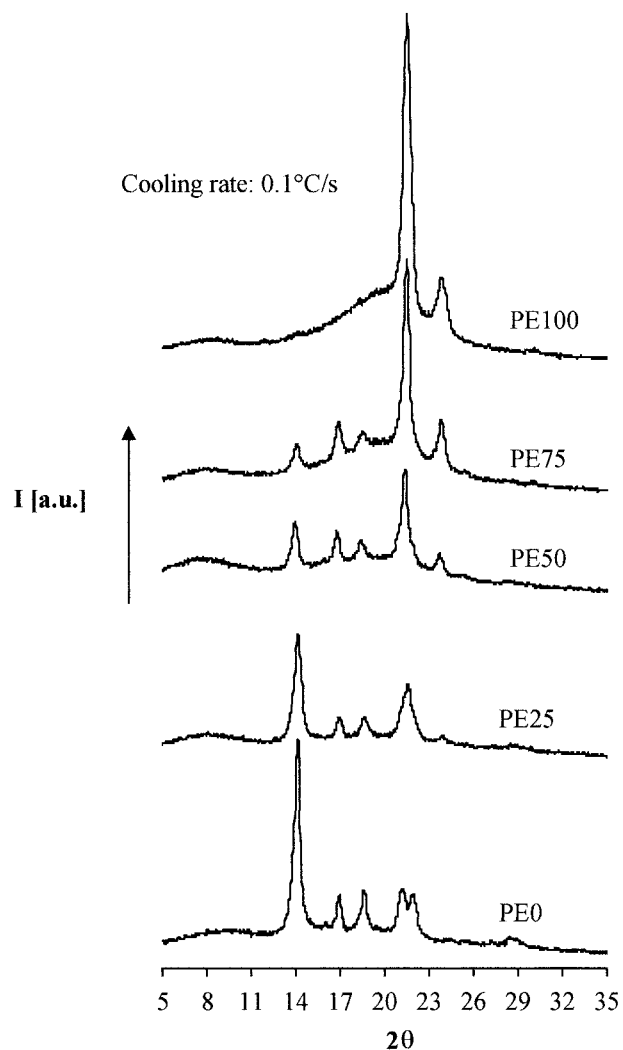
Figure 3 X-ray diffractograms of samples solidified at a slow cooling rate.

iPP and LLDPE crystallize independently in their usual crystalline forms and any kind of cocrystallization is excluded. The WAXDs of the same materials submitted to fast cooling (500°C/s) are reported in Figure 4. With this processing condition, while the pure LLDPE appears crystalline in the usual orthorhombic cell, the pure iPP is in the smectic form, as always found for iPP submitted to rapid cooling from the melt.[19] The diffractograms of the blends deserve particular attention, in particular, toward the iPP behavior. Indeed, iPP appears smectic in the blend fPE25-PP75, but, when its percentage decreases (samples fPE50-PP50 and fPE75-PP25), it shows a relevant degree of monoclinic α crystallinity. This is an indication that the α crystallization of iPP is enhanced by the presence of LLDPE (at a concen-

tration of 50% or more) and can take place even at drastic cooling conditions.

Sample densities measured at 25°C are shown in Figure 5, versus the blend composition. Density changes about linearly with composition for both cooling rates. This could be taken as a further indication that the final crystallinity degree for both materials is not strongly dependent upon the blend composition. The enhancement effect of LLDPE on iPP crystallization, taking place at low iPP percentages, falls below the resolution power of densitometry due to the relatively small difference between the densities of monoclinic α and smectic forms. The effect of the cooling rate is clearly shown in the diagram: samples solidified at the lowest cooling rate have higher densities
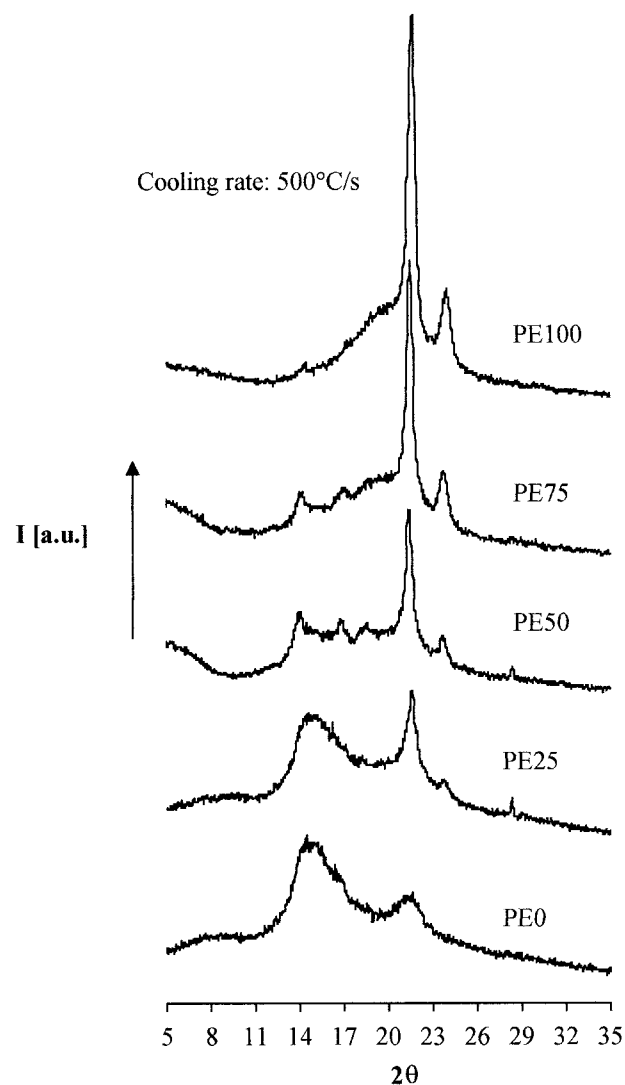

Figure 4 X-ray diffractograms of samples solidified at a high cooling rate.
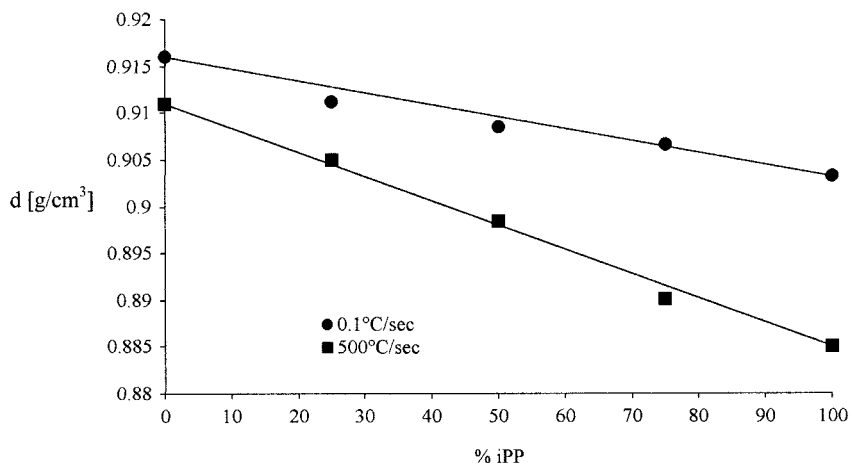
Figure 5   Density measurements performed at 25°C 1 h after solidification.

with respect to those solidified at 500°C/s. As expected, due to the faster crystallization kinetics, the effect of the cooling rate is less relevant for LLDPE, whereas the density of iPP substantially reduces it if it solidifies at high cooling rates.

Transport Properties

The penetrant concentration at the time t, C_t, divided by the equilibrium concentration C_{eq}, was plotted as a function of the square root of time. The sorption curves determined at each vapor activity showed a Fickian behavior, so that it was possible to derive an average diffusion coefficient, $\bar{D}$, for each vapor concentration using the following relationship[20]:

$$\frac{C_t}{C_{eq}} = \frac{4}{d}\left(\frac{\bar{D}t}{\pi}\right)^{1/2} \tag{1}$$

where d [cm] is the thickness of the sample.

The average diffusion parameter is not constant at each vapor activity, but increases with increasing vapor concentration; it is therefore important to determine the dependence of the diffusion on the concentration, to extrapolate to zero penetrant concentration, and obtain the thermodynamic parameter, Do, which is related to the fractional free volume present in the system. Generally, the dependence is of the exponential form[21]:

$$\bar{D} = Do \, \exp(\gamma C_{eq}) \tag{2}$$

where γ is the concentration coefficient also related to the fractional free volume, and to the effectiveness with which the penetrant plasticizes the polymer.

Figure 6 reports the values of the Do coefficients, as a function of the iPP concentration, for all the films after the two cooling processes. It is very interesting to note that, using a slow cooling rate (0.1°C/s), the decrement of Do [cm²/s] from the pure LLDPE value to the pure iPP value is relevant already at 25% of iPP, suggesting an "inversion" of the amorphous permeable phase from a "polyethylenic" type to a "polypropylenic" one, already with the addition of 25% of iPP. The situation appears quite different at high cooling rates (500°C/s). In this condition, the value of Do follows a more gradual decrement from the pure LLDPE to the pure iPP, suggesting a different morphological organization of the two amorphous phases that is strictly related to the thermal history.
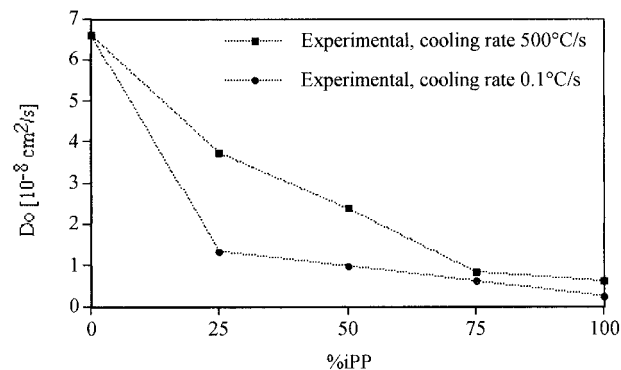

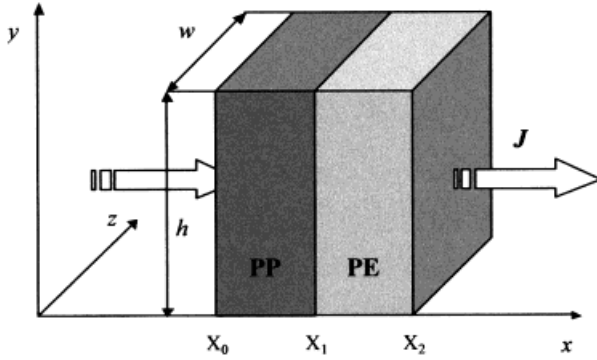**Figure 6**   Experimental values of Do.

Figure 7 Model considering the two polymers in series with respect to the mass flux, J.

Modeling Material Resistance to Diffusion

Following a common approach in modeling composites' properties, it can be assumed that the type of morphology of the amorphous phases of the two materials has a resistance to diffusion which is intermediate between the two idealized samples depicted in Figures 7 and 8, representing the two components combined in series and in parallel, respectively, with respect to vapor diffusion (these two combinations are usually referred to as Pauli's limits). The evaluation of the diffusion coefficient for the two configurations is performed as follows:

Elements in Series

In this case, depicted in Figure 7, vapor diffusion encounters both resistances. The two phases are described as layers having a thickness, x, which is proportional to their volume fraction, indicated with "f" in the following (which nearly corresponds to the mass fraction). By integrating the equation

$$J = -D \frac{\partial C}{\partial x} \tag{3}$$

(in which J is the mass flux; D, the diffusion coefficient; and C, the vapor concentration), one simply gets

$$\Delta C = -J \left[\frac{X_1 - X_0}{D_{iPP}} + \frac{X_2 - X_1}{D_{PE}} \right] \tag{4}$$

(the symbol Δ refers to "2"–"0"), which can be rearranged, giving

$$-\frac{1}{J} \frac{\Delta C}{\Delta X} = \frac{1}{D_{series}} = \frac{X_1 - X_0}{\Delta X D_{iPP}} + \frac{X_2 - X_1}{\Delta X D_{PE}} \tag{5}$$

being

$$\frac{X_1 - X_0}{\Delta X} = f_{iPP} \quad \text{and} \quad \frac{X_2 - X_1}{\Delta X} = f_{PE}$$

The resulting overall diffusion coefficient is

$$D_{series} = \frac{1}{\dfrac{f_{iPP}}{D_{iPP}} + \dfrac{f_{PE}}{D_{PE}}} \tag{6}$$

Equation (6) clearly shows that, in this configuration, the controlling mechanism is the diffusion through the material having the largest resistance to mass flow.

Elements in Parallel

The two phases are described in Figure 8 as layers having the outer surfaces, A, proportional to their volume fraction (nearly corresponding to the mass fraction).

The total flux through the two layers can be described as

$$JA = J_{iPP}A_{iPP} + J_{PE}A_{PE} \tag{7}$$

Following the same calculating procedure as for the configuration in series, one simply gets

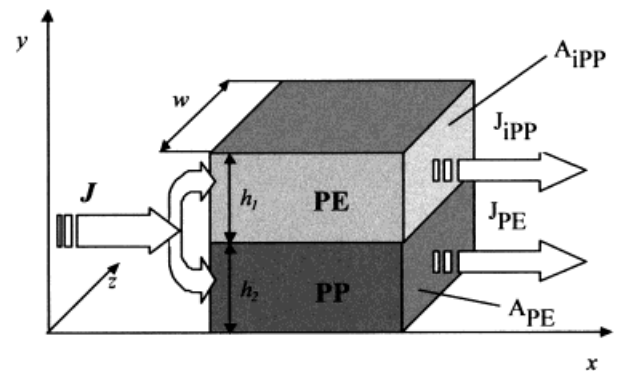$$D_{parallel} = f_{iPP}D_{iPP} + f_{PE}D_{PE} \tag{8}$$

Figure 8 Model considering the two polymers in parallel with respect to the mass flux, J.

Comparison with Experimental Results

Results of eqs. (6) and (8) are compared in Figure 9 with the experimental data of the diffusion coefficient. A comparison clearly shows that the diffusivity of the samples cooled at a "slow" cooling rate (0.1°C/s) is well described by the model in series. At higher cooling rates (500°C/s), the experimental data appear to be better-fitted by the other Pauli's limit (model in parallel). Indeed, to obtain a best fit of these experimental data, a combination (a parallel) of the configurations depicted above was used. According to this scheme, reported in Figure 10, the resulting overall diffusion coefficient is

$$D_{\text{overall}} = aD_{\text{parallel}} + (1-a)D_{\text{series}} = \frac{a}{\dfrac{f_{\text{iPP}}}{D_{\text{iPP}}} + \dfrac{f_{\text{PE}}}{D_{\text{PE}}}}$$
$$+ (1-a)(D_{\text{iPP}}f_{\text{iPP}} + D_{\text{PE}}f_{\text{PE}}) \quad (9)$$

where a (ranging from 0 to 1) represents the percentage of the total blend volume combined in series (upper portion in Figure 10). Of course, if $a = 0$ or $a = 1$, the two Pauli's limits are described. As is clear from Figure 9, where the comparison with the experimental data is shown, when $a = 50\%$, this last combination allows a satisfactorily fit of the experimental data relative to samples solidified at high cooling rates.

CONCLUSIONS

The structural organization of blends iPP/LLDPE at different compositions was studied for two thermal histories: a "slow" cooling, with cooling
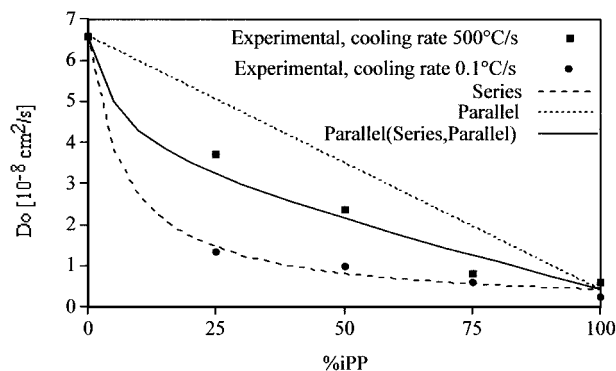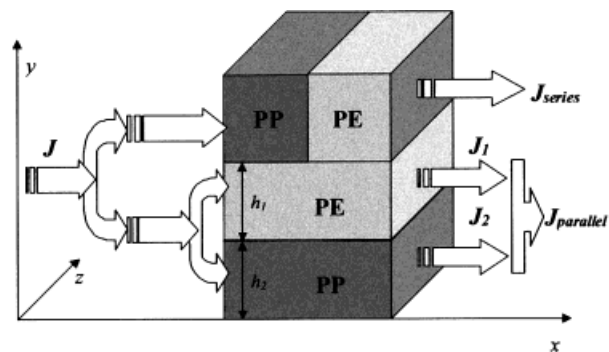

Figure 10 Model considering the two polymers in a more complex parallel model, composed of (upper part of the figure) a series of both and (lower part of the figure) a parallel of both, in respect to mass flux, J.

rates of about 0.1°C/s (in the temperature interval 70–100°C), and a "fast" cooling, reaching about 500°C/s. Diffractometric analysis showed that iPP and LLDPE independently crystallize in their usual crystalline forms, that is, monoclinic or smectic (depending on the cooling) for the first and orthorhombic for the second. At the "high" cooling rate, it was found from X-ray analysis that the presence of LLDPE with a composition higher than 50% enhances the crystallization of iPP in the monoclinic form, rather than in the smectic one.

The diffusion parameters, related to the amorphous fractions, showed that for the slowly cooled blends, already at a composition of 25% of iPP, the diffusion is very similar to that of pure PP. At high cooling rates, the value of Do follows a more gradual decrement from the 100% LLDPE to the 100% iPP, suggesting a different morphological organization of the two amorphous phases, which, thus, seems to be strictly related to the thermal history.

The results of the diffusion parameters for the slowly cooled samples could be well described, considering the amorphous phases of the two materials as resistances to diffusion combined in series. This indicates that the controlling mechanism is the diffusion through the material having the largest resistance to mass flow. For the blends cooled with a high cooling rate, the experimental data could be well described, considering the amorphous phases of the two materials as resistances to diffusion combined in a slightly more complex way.

Figure 9 Comparison between experimental and simulated values of Do.

Progetto Finalizzato Materiali Speciali per Tecnologie Avanzate II.

REFERENCES

1. Saiu, M.; Brucato, V.; Piccarolo, S.; Titomanlio, G. Int Polym Proc 1992, 7, 3.
2. Piccarolo, S.; Saiu, M.; Brucato, V.; Titomanlio, G. J Appl Polym Sci, 1992, 46, 625.
3. Favis, B. D. J Appl Polym Sci 1990, 39, 285.
4. Min, K.; White, J. L. Fellers, J. F. Polym Eng Sci 1984, 24, 1327.
5. Van Gheluwe, P.; Favis, B. D.; Chalifoux, J. P. J Mater Sci 1988, 23, 3910.
6. Hopfenberg, H. B.; Paul, D. R. In Polymer Blends; Paul, D. R.; Newman, S., Eds.; Academic: New York, 1978; Chapter 10, p 445.
7. Noel, F.; Carley, J. F. Polym Eng Sci 1975, 15, 177.
8. Janimak, J.; Cheng, S.; Zhang, A.; Hsieh, E. Polymer 1992, 33, 728.
9. Avalos, F.; Lopez-Manchado, M.; Arroyo, M. Polymer 1996, 37, 5681.
10. Olley, R. H.; Hodge, M. A.; Bassett, D. C. J Polym Sci Phys 1979, 17, 627.
11. Lovinger, A. J.; Williams, M. L. J Appl Polym Sci 1980, 25, 1703.
12. McBrierty, V. J.; Douglass, D. C.; Barham, P. J. J Appl Polym Sci 1980, 18, 1561.
13. Bartlett, D. W.; Barlow, J. W.; Paul, D. R. J Appl Polym Sci 1982, 27, 2351.
14. Peterlin, A. J Macromol Sci Phys 1975, 11, 57.
15. Michaels, A. S.; Wieth, W. R.; Barrie, J. J Polym Sci Phys 1975, 11, 57.
16. Vittoria, V.; de Candia, F.; Capodanno, V.; Peterlin, A. J Polym Sci Phys 1986, 24, 1009.
17. D'Aniello, C.; Guadagno, L.; Gorrasi, G.; Vittoria, V. Polymer 2000, 41, 2515.
18. Pantani, R.; Titomanlio, G. J Appl Polym Sci 2001, 81, 267.
19. Natta, G.; Peraldo, M.; Corradini, P. Rend Acc Naz Lincei 1959, 26, 14.
20. Crank, J. The Mathematics of Diffusion; Oxford University: 1967; Chapter IV, p 352.
21. Fujita, H. Diffusion in Polymer Diluent Systems; Crank, J.; Park, G. S.; Eds.: Academic: New York, 1968; pp 1–17.